Sustained diffusive alternating current gliding arc discharge in atmospheric pressure air

Zhu, Jiajian; Gao, Jinlong; Li, Zhongshan; Ehn, Andreas; Aldén, Marcus; Larsson, Anders; Kusano, Yukihiro

Published in:
Applied Physics Letters

DOI:
10.1063/1.4903781

2014

AIP | Applied Physics Letters

Sustained diffusive alternating current gliding arc discharge in atmospheric pressure air

Jiajian Zhu, Jinlong Gao, Zhongshan Li, Andreas Ehn, Marcus Aldén, Anders Larsson, and Yukihiro Kusano

Citation: Applied Physics Letters **105**, 234102 (2014); doi: 10.1063/1.4903781
View online: http://dx.doi.org/10.1063/1.4903781
View Table of Contents: http://scitation.aip.org/content/aip/journal/apl/105/23?ver=pdfcov
Published by the AIP Publishing

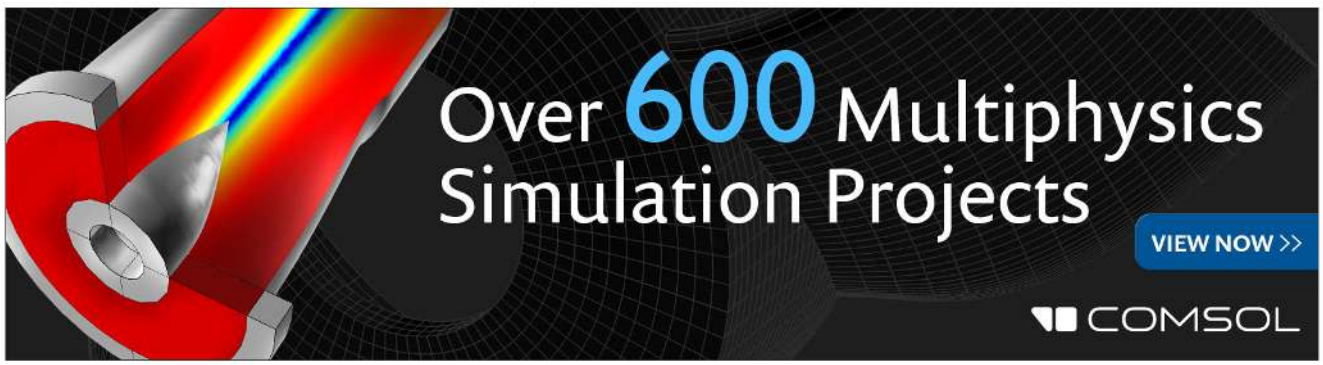

Sustained diffusive alternating current gliding arc discharge in atmospheric pressure air

Jiajian Zhu,[1] Jinlong Gao,[1] Zhongshan Li,[1,a)] Andreas Ehn,[1] Marcus Aldén,[1] Anders Larsson,[2] and Yukihiro Kusano[3]
[1]*Division of Combustion Physics, Lund University, P.O. Box 118, S-221 00 Lund, Sweden*
[2]*Swedish Defence Research Agency, SE-164 90 Stockholm, Sweden*
[3]*Department of Wind Energy, Section for Composites and Materials Mechanics, Technical University of Denmark, Risø Campus, Frederiksborgvej 399, DK-4000 Roskilde, Denmark*

(Received 6 October 2014; accepted 26 November 2014; published online 10 December 2014)

Rapid transition from glow discharge to thermal arc has been a common problem in generating stable high-power non-thermal plasmas especially at ambient conditions. A sustained diffusive gliding arc discharge was generated in a large volume in atmospheric pressure air, driven by an alternating current (AC) power source. The plasma column extended beyond the water-cooled stainless steel electrodes and was stabilized by matching the flow speed of the turbulent air jet with the rated output power. Comprehensive investigations were performed using high-speed movies measured over the plasma column, synchronized with simultaneously recorded current and voltage waveforms. Dynamic details of the novel non-equilibrium discharge are revealed, which is characterized by a sinusoidal current waveform with amplitude stabilized at around 200 mA intermediate between thermal arc and glow discharge, shedding light to the governing mechanism of the sustained spark-suppressed AC gliding arc discharge. © *2014 AIP Publishing LLC*.
[http://dx.doi.org/10.1063/1.4903781]

Non-thermal plasmas for industrial applications, e.g., glow discharges[1] and radio frequency discharges,[2] are generally developed at low-pressure. However, the requirement of expensive and complicated vacuum systems forms the main drawback.[3] Many techniques, e.g., corona,[4] dielectric barrier discharge (DBD),[5] and arc discharge,[6] have been developed to be applied at atmospheric pressure. However, corona and DBD produce extremely small current and limit to restricted discharge area.[7] Arc discharge can provide high operating power, but it is regarded unfavorable due to its nature of thermal plasma.[6,7] Gliding arc has been recognized to provide high operating power in non-thermal conditions at atmospheric pressure.[8–15] Nevertheless, the reported gliding arcs generally suffer from limited existing period[16] and volume.[17] In this letter, we report on comprehensive investigations of a sustained diffusive alternating current (AC) gliding arc with large volume and high power.

In our previous works,[18–20] we found that the performance of an AC gliding arc was affected by the turbulent intensity of the gas flow. Among the frequent transition from the glow-type to the spark-type discharge, there probably exists a fragile balance between the input electric power and the convective cooling of the plasma column by the turbulent gas flow. Assuming a fixed input electric power, a too high flow rate causes more intensive turbulence and thereby cooling of the discharge channel, promoting quenching, and re-ignition. A too low flow rate will limit the production rate of active species. Thus, there is an optimal flow rate to form a diffusive gliding arc discharge within a larger volume, and the selected input electric power partially determines the optimal flow rate. However, the governing mechanism of the gliding arc is still unknown and comprehensive diagnostics are required. In this study, a sustained diffusive gliding arc was obtained by matching the rated output power with the air flow rate, and the physical property was investigated by recording the current and voltage waveforms in synchronization with high-speed movies. The electrical field strength, discharge length, active power, and impedance of the plasma column were analyzed, and the electron temperature and density were evaluated to gain a better understanding of the governing mechanism of the discharge.

Fig. 1 shows a photo of a diffusive gliding arc and a schematic of the experimental setup. The gliding arc was generated using a 35 kHz AC power supply (9030E,

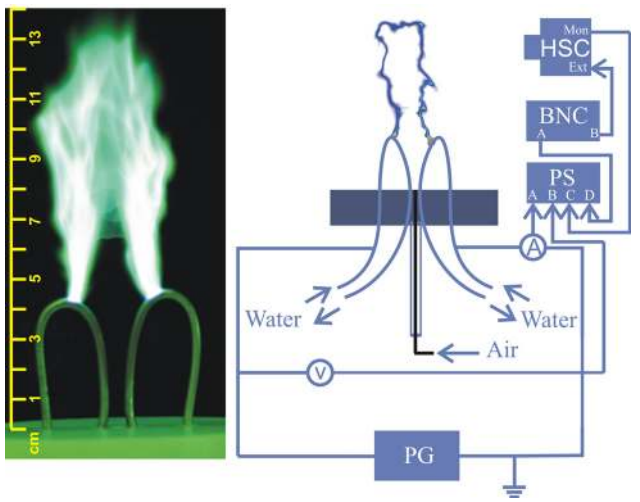

FIG. 1. A photo of the gliding arc (1/30 s exposure time) and a schematic of experimental setup. PG: power generator; PS: PicoScope (4-channel oscilloscope); and BNC: pulse generator.

[a)]Email: Zhongshan.li@forbrf.lth.se

SOFTAL Electronic GmbH, Germany, rated power 1200 W), stainless steel electrodes, and turbulent air flows. The hollow tubular electrodes with an outer diameter of 3 mm are internally water-cooled. An air flow is supplied from an air compressor through a 3-mm diameter hole between the two electrodes with a flow rate of 17.5 standard liter per minute, giving an exit speed of about 40 m/s. A similar gliding arc system has been described in detail in our previous work.[18–20] A high framing-speed camera (HSC, Fastcam SA-X2, Photron) equipped with an objective lens (Micro-Nikkor 105 mm, f/2.8) was employed to capture the dynamics of the gliding arc. Measurements were performed at a frame rate of 20 kHz with an exposure time of 16.25 μs and a resolution of 1024×512 pixels. A current monitor (model 6585, Pearson Electronics) and a voltage probe (Tektronix P6015A) were used for current and voltage waveform measurements. The current and voltage signal together with the HSC gate and the external trigger were recorded simultaneously using a four channels oscilloscope (PicoScope 4424, PS). The PS and the HSC were externally triggered by a pulse generator (BNC 575).

Fig. 2 shows a typical voltage and current waveform of the gliding arc recorded at a time span of 180 ms. Note that the gliding arc can be sustainably operated in such a condition. Both the recorded voltage and current waveforms show a uniform sawtooth-like envelope with a time period of a few milliseconds. The peak voltage varies from about 3 to 12 kV, while the current is close to 0.2 A except for a few sharp spikes. Generally, the voltage is constantly increasing, whilst the current decreases to response to the rated output power of the power supply. Occasionally, there exist several spikes in the current waveform and these current peaks can be categorized into three different types, represented by the regions marked by *b*, *c*, and *d* in Fig. 2.

Fig. 3 shows the detailed voltage and current waveforms marked by *a*, *b*, c, and *d* in Fig. 2 as well as the corresponding synchronized camera gates as positive squares. Fig. 3(a) represents the current and voltage waveforms in the majority part of the time, where the voltage is a sinusoidal waveform with a peak value of 8 kV and has the same frequency of 35 kHz as the AC power supply, and the current is slightly

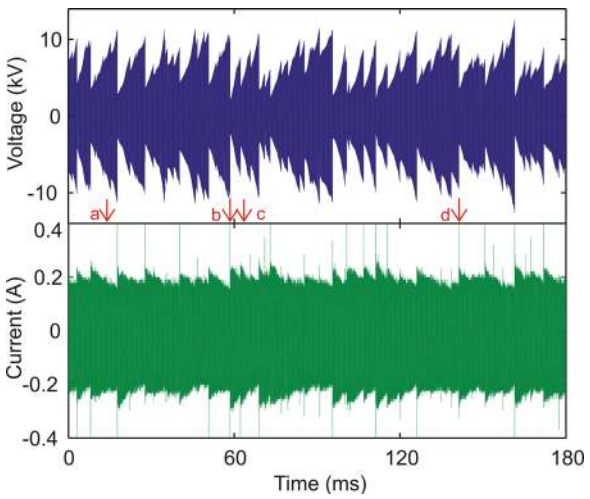

FIG. 2. Voltage and current waveforms of the gliding arc at a time span of 180 ms. Details of the waveforms marked by a, b, c, and d are shown in Fig. 3.

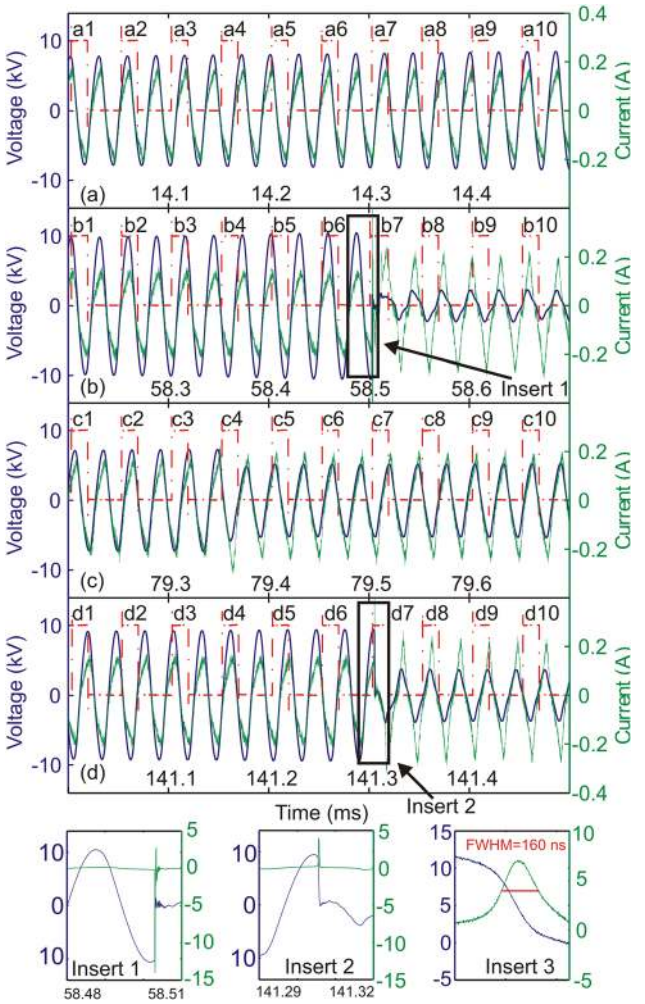

FIG. 3. Detailed voltage-current waveform marked by a, b, c, and d in Fig. 2 together with the camera gates. The current peaks in (b) and (d) were displayed as inset 1 and 2 at the bottom row. Inset 3 shows a typical peak current width.

deformed but still close to a sinusoidal waveform. The impedance of the plasma channel, which increases with plasma column length, introduces a slight phase shift between the current and the voltage. This phase shift is negligible, indicating an efficient electric energy transfer to the plasma column. The regular current and voltage waveforms also imply that the discharge is stable and free from breakdown or short-cutting events. Instantaneous images of the gliding arc synchronized with the current and voltage measurements are shown in Fig. 4(a). These images, *a*1–*a*10, correspond to the 10 camera gates shown in Fig. 3(a) and reveal a plasma column with a projected length of about 19 cm, which is obtained by analyzing individual images of the plasma column taken by the high speed camera.

Fig. 3(b) shows an abrupt change in current and voltage at 58.5 ms. The peak of the current is illustrated as inset 1 in the bottom row of Fig. 3. The current is approaching 15 A and recovers to show a sinusoidal-like waveform with slightly bigger amplitude after the instantaneous high-current peaks. The voltage waveform is distorted for about 15 μs and then recovers back to sinusoidal waveforms with a smaller peak value. An oscilloscope with a sample rate of 2 GS/s (Tektronix TSD 380) was used to record the transient

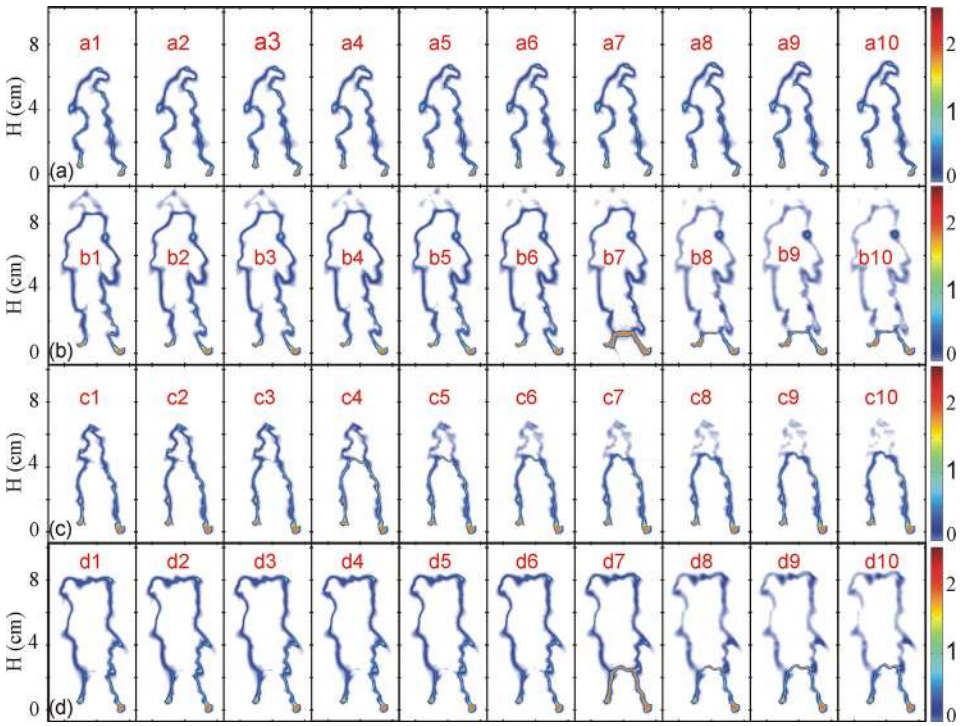

FIG. 4. Instantaneous images of gliding arc recorded simultaneously with the current and voltage waveform shown in Fig. 3. The images were acquired with a framing speed of 20 kHz and an exposure time of 16.25 μs.

of the high-current peak, and the full width at half maximum is found to be about 160 ns as shown in the inset 3. The instantaneous gliding arc images around the high peak current event are shown in Fig. 4(b), which reveal that a breakdown near the plasma anchor points has short-cut the majority of the plasma column. The instantaneous breakdown at *b*7 of Fig. 4(b) may be understood by these facts: (1) a breakdown takes place where the plasma columns have the narrowest gap; (2) there is a large proportion of diffusive active species formed close to the breakdown channel, before the breakdown takes place, which further promote the breakdown formation although the electric field strength is smaller than the value of air breakdown (3 MV/m) at atmospheric pressure;[11] and (3) the exposure gate-time of the bright image shown at *b*7 in Fig. 4(b) covered the high peak transient current, which is obviously introduced by the shock of the sudden reduction of the impedance from the short-cut of the plasma column.

It can be seen from Fig. 3(c) that a slight increase of the amplitude of the current waveform occurs at about 79.38 ms, which corresponds to another short-cutting event as illustrated in Fig. 4(c-*c*4). However, no breakdown characterized by a spike current was found due to the fact that the short-cutting length is much smaller than that happened in Fig. 4(b). In Fig. 3(d), a current peak was identified and the amplitude of the current is about 4 A. Similarly, a breakdown event shown in Fig. 4(d-*d*7) was recognized due to the large short-cutting length and a significant voltage drop. In summary, high current peaks (>1 A) are always associated with bigger short-cutting length, while small peaks (<0.4 A) correspond to smaller short-cutting length. These breakdown-induced short-cutting events are unfavorable since it not only intends to turn the plasma column to a thermal discharge but also shortens the plasma column. However, only tens of the narrow high current peaks were found within 180 ms. Furthermore, during the operation of the gliding arc, there is no new ignition at the narrowest electrodes gap as observed most of the time for other reported gliding arcs.[8,13,23]

Fig. 5 shows the dependence of active power and impedance of the plasma column on the measured projected length of the gliding arc discharge column. Each point of the active power was calculated from the current and voltage data covering each camera gate time as given by

$$P = \frac{1}{t_2 - t_1}\int_{t_1}^{t_2} V(t)I(t)dt, \tag{1}$$

where t_1 and t_2 represent the time of open and close of the camera gate. Each point of the impedance was calculated using the ratio of root-mean-square (RMS) of the voltage value and the RMS of current value during each camera

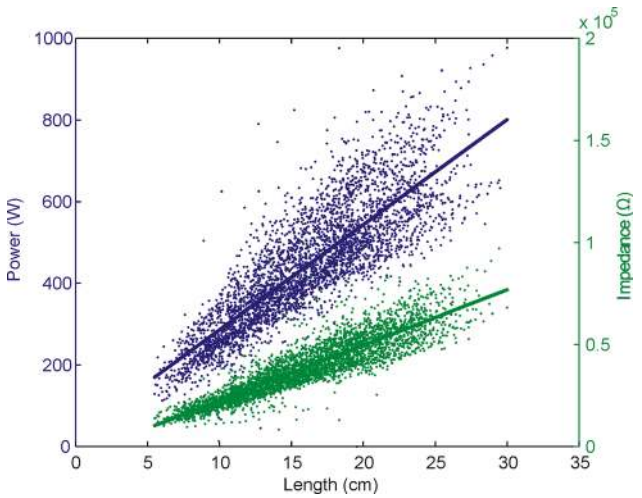

FIG. 5. Dependence of active power and impedance on the projected length of the plasma column.

gate. Both the active power and impedance linearly increase with the plasma column length, and the fitted lines were indicated in Fig. 5, resulting in a power per length of about 2.6 kW/m and a impedance of about 270 kΩ/m. Similarly, the voltage per unit length, namely, electric field strength, is estimated to be 26 kV/m. These characteristic parameters make the diffusive gliding arc different from both thermal arc[16] and weak glowing-type discharges.[17] Furthermore, the diffusive arc length is up to 25 cm, which is 5–10 cm longer than gliding arc discharges reported previously.[9,14] The power dissipated in the plasma column is about 700 W when the plasma column has a length of 25 cm. Note that the dispersion of measurements in Fig. 5 increases with the length of the plasma column. This is mainly because the projected 2D length of the plasma column differs more from the real 3D length for longer plasma channels.

By following the analysis by Korolev *et al.*[21] and assuming glow discharge conditions at the cathode, the gas temperature can be estimated by the empirical formula:

$$T = (240 \times 10^{-6} P_0^2 T_0^2 / j)^{0.5} \text{ K}, \quad (2)$$

where $P_0 = 760$ Torr, $T_0 = 300$ K, and j is the current density at the cathode spot with an unit of A/cm^2. The cathode spot diameter is measured to be 0.24 cm and the current is 0.2 A, giving a current density of 4.4 A/cm^2. With this, the gas temperature is estimated to be about 1680 K. Electron temperature and electron density of the gliding arc are important parameters, and an estimation of these parameters can be achieved using BOLSIG$^+$ Boltzmann solver[22] with the input of the reduced electric field strength and gas composition. The reduced electrical field strength is around 6 Td calculated using the measured electric field strength 26 kV/m and the estimated gas temperature 1680 K, yielding an estimate of the electron temperature of 0.8 eV (9000 K). The big difference between the gas temperature and the electron temperature implies that the gliding arc was running at a high degree of non-thermal equilibrium. The electron density can be estimated using

$$n_e = j/(\mu E e), \quad (3)$$

where j is current density, $\mu = 1.45$ m^2/V/s is mobility (from BOLSIG$^+$ simulation), E is electric field strength, and e is elementary charge, yielding an electron density of 7.3×10^{18} m^{-3}.

In summary, we demonstrate a sustained diffusive spark-suppressed AC gliding arc, which can be run at non-thermal conditions with high power and large volume, with a dissipation of 2.6 kW/m of electric energy along the discharge channel. The simultaneously recorded current and voltage waveform together with high-speed movies provide unprecedented details of the physical properties of the highly dynamic processes. The gas temperature in the plasma column is estimated to be 1680 K, while the electron temperature is estimated to be about 9000 K (0.8 eV) and electron number density is about 7.3×10^{18} m^{-3}. The governing mechanism for the formation of the diffusive gliding arc discharge can be explained by the interaction between the turbulent convection and the plasma column, which plays key roles in sustaining the diffusive gliding arc. First, turbulent convections continually dissipate heat and active radicals out of the plasma column while input electric power provides energy to sustain the plasma column, and energetic balance between the heat dissipated in the plasma column and the turbulent convection may be maintained, which together with the limited output power of the AC power supply prevent the transition from glow-type discharge to thermal arc. Second, the twist of the plasma column and the transportation of active species and ions introduced by the turbulent flow give the possibility of sequentially short-cutting of the plasma column to avoid re-ignition. Besides, the long-lived metastable states and radicals generated in the plasma column will aid in sustaining a diffusive discharge when the voltage from the AC power supply recovered after some shocks of peak breakdown currents introduced by, e.g., short-cutting events. A comprehensive numerical modeling including the turbulent convection and plasma chemistry is required to provide quantitative understanding of this novel gliding arc discharge.

The work was financially supported by the Swedish Energy Agency, Swedish Research Council (VR), Knut & Alice Wallenberg Foundation, and European Research Council. J. Zhu and J. Gao would like to thank China Scholarship Council for financial support.

[1]G. W. Mcclure, Appl. Phys. Lett. **2**(12), 233–234 (1963).
[2]M. Y. Pustylnik, L. Hou, A. V. Ivlev, L. M. Vasilyak, L. Couedel, H. M. Thomas, G. E. Morfill, and V. E. Fortov, Phys. Rev. E **87**(6), 063105 (2013).
[3]J. Park, I. Henins, H. W. Herrmann, G. S. Selwyn, J. Y. Jeong, R. F. Hicks, D. Shim, and C. S. Chang, Appl. Phys. Lett. **76**(3), 288–290 (2000).
[4]D. S. Antao, D. A. Staack, A. Fridman, and B. Farouk, Plasma Sources Sci. Technol. **18**(3), 035016 (2009).
[5]L. F. Dong, Y. Z. Zhang, W. Y. Liu, L. Yang, and J. Y. Chen, Appl. Phys. Lett. **94**(9), 091502 (2009).
[6]A. Blais, P. Proulx, and M. I. Boulos, J. Phys. D: Appl. Phys. **36**(5), 488–496 (2003).
[7]A. Schutze, J. Y. Jeong, S. E. Babayan, J. Park, G. S. Selwyn, and R. F. Hicks, IEEE Trans. Plasma Sci. **26**(6), 1685–1694 (1998).
[8]F. Richard, J. M. Cormier, S. Pellerin, and J. Chapelle, J. Appl. Phys. **79**(5), 2245–2250 (1996).
[9]V. Dalaine, J. M. Cormier, and P. Lefaucheux, J. Appl. Phys. **83**(5), 2435–2441 (1998).
[10]A. Fridman, S. Nester, L. A. Kennedy, A. Saveliev, and O. Mutaf-Yardimci, Prog. Energy Combust. Sci. **25**(2), 211–231 (1999).
[11]O. Mutaf-Yardimci, A. V. Saveliev, A. A. Fridman, and L. A. Kennedy, J. Appl. Phys. **87**(4), 1632–1641 (2000).
[12]S. Pellerin, F. Richard, J. Chapelle, J. M. Cormier, and K. Musiol, J. Phys. D: Appl. Phys. **33**(19), 2407–2419 (2000).
[13]X. Tu, L. Yu, J. H. Yan, K. F. Cen, and B. G. Cheron, Phys. Plasmas **16**(11), 113506 (2009).
[14]Z. B. Feng, N. Saeki, T. Kuroki, M. Tahara, and M. Okubo, Appl. Phys. Lett. **101**(4), 041602 (2012).
[15]Z. Bo, E. K. Wu, J. H. Yan, Y. Chi, and K. F. Cen, Rev. Sci. Instrum. **84**(1), 016105 (2013).
[16]A. Larsson, L. Adelöw, M. Elfsberg, and T. Hurtig, IEEE Trans. Plasma Sci. **42**(10), 3186–3190 (2014).
[17]C. Zhang, T. Shao, J. Y. Xu, H. Ma, L. W. Duan, C. Y. Ren, and P. Yan, IEEE Trans. Plasma Sci. **40**(11), 2843–2849 (2012).
[18]J. J. Zhu, Z. W. Sun, Z. S. Li, A. Ehn, M. Alden, M. Salewski, F. Leipold, and Y. Kusano, J. Phys. D: Appl. Phys. **47**(29), 295203 (2014).
[19]Z. W. Sun, J. J. Zhu, Z. S. Li, M. Alden, F. Leipold, M. Salewski, and Y. Kusano, Opt. Express **21**(5), 6028–6044 (2013).

[20]Y. Kusano, B. F. Sorensen, T. L. Andersen, H. L. Toftegaard, F. Leipold, M. Salewski, Z. W. Sun, J. J. Zhu, Z. S. Li, and M. Alden, J. Phys. D: Appl. Phys. **46**(13), 135203 (2013).
[21]Y. D. Korolev, O. B. Frants, V. G. Geyman, N. V. Landl, and V. S. Kasyanov, IEEE Trans. Plasma Sci. **39**(12), 3319–3325 (2011).
[22]G. J. M. Hagelaar and L. C. Pitchford, Plasma Sources Sci. Technol. **14**(4), 722–733 (2005).
[23]See supplementary material at http://dx.doi.org/10.1063/1.4903781 for a movie showing the dynamics of the gliding arc as well as the simultaneously recorded current and voltage waveforms.